Skin damage mechanisms related to airborne particulate matter exposure

Natalia D. Magnani[1], Ximena M. Muresan[2], Giuseppe Belmonte[2], Franco Cervellati[2], Claudia Sticozzi[2], Clelia Miracco[3], Timoteo Marchini[1], Pablo Evelson[1], Giuseppe Valacchi[2-4*]

[1] Institute of Biochemistry and Molecular Medicine (IBIMOL-UBA-CONICET), Pharmacy and Biochemistry School, University of Buenos Aires, Buenos Aires, Argentina.

[2]Department of Life Sciences and Biotechnology, University of Ferrara, Ferrara, Italy

[3]Department of Neuroscience, Medical and Surgical Sciences. University of Siena, Siena, Italy

[4]Department of Human Nutrition, Kyung Hee University, Seoul, South Korea

Running Title: Airborne particle affect skin tissues

***Corresponding Author:**

Prof. Giuseppe Valacchi, PhD

Department of Life Sciences and Biotechnology,

University of Ferrara, Ferrara, Italy

Via Borsari, 46, Ferrara, Italy

Tel.: +39-0532/455482

Email: vlcgpp@unife.it

Abstract

Epidemiological studies suggest a correlation between increased airborne particulate matter (PM) and adverse health effects. The mechanisms of PM-health effects are believed to involve oxidative stress and inflammation. To evaluate the ability of PM promoting skin tissue damage, the main organ exposed to outdoor pollutants, we analyzed the effect of Concentrated Ambient particles (CAPs) in a Reconstructed Human Epidermis (RHE) model. RHE tissues were exposed to 25 or 100 µg/mL CAPs for 24 or 48 hrs. Data showed that RHE seems to be more susceptible to CAPs-induced toxicity after 48 hrs exposure. A local reactive O_2 species (ROS) production increase could be generated from metals present on the particle, and contribute to lipids oxidation. Furthermore, as a consequence of altered redox status, NFkB nucleus translocation was increase upon CAPs exposure, as well as COX2 and CYP levels, which may be involved in the inflammatory response initiated by PM. CAPs also triggered an apoptotic process in skin. Surprisingly, by TEM analysis we have showed that CAPs were able to penetrate skin tissues. These findings contribute to the understanding of the cutaneous pathophysiological mechanisms initiated by CAPs exposure, where oxidative stress and inflammation may play predominant roles.

Keywords: air pollution, cutaneous tissues, particulate matter, oxidative damage, inflammation

List of abbreviations

PM, particulate matter

CAPs concentrates air particles

LDH Lactate dehydrogenase

ROS Reactive Oxygen Species

SEM scanning electron microscopy

IsoPro isoprostanes

4-HNE 4-hydroxynonenal

CYP citochorme P450

IL-1 interleukin 1

COX2 cyclooxygenase 2

TUNEL Terminal deoxynucleotidyl transferase-mediated deoxyuridine triphosphate nick end labelling

TEM transmission electron microscopy

Introduction

Numerous studies have shown a direct correlation between decreased air quality levels and adverse health effects (Brunekreef and Holgate, 2002; Valacchi *et al*., 2012). Air pollution is a heterogeneous mixture of chemicals and solid particles, in which both organic and inorganic compounds could be found in the particle's core as well as in the surface. They are emitted into the atmosphere from natural and anthropogenic sources. Among the wide variety of pollutants, particulate matter (PM), specially particles on the nanosize range, seems to be of major concern from a health perspective, and has been pointed out as an environmental threat not only to susceptible but also to healthy members of the population (WHO, 2012). Airborne PM is comprised of a mixture of solid and liquid particles, in which chemical composition, size and sources of origin differ in each microenvironment (Nel, 2005).

Concentrated Air Particles (CAPs) represent the fine and ultrafine fraction of atmospheric pollutants collected by a particle concentrator. Therefore, CAPs have the advantage of allowing "real world PM" exposures (Ghio and Huang, 2004).

The respiratory and oral tracts along with the skin are the common routes by which organisms enter in contact with different ambient pollutants. Because of its critical location, the skin provides a major interface between the body and the environment, and offers a biological barrier against air PM (Valacchi *et al.*, 2012). However, the skin defensive capacity is not unlimited. Environmental stressors may exceed the protective potential and disturb the skin structure leading to skin diseases, such as erythema, edema, hyperplasia, skin aging, contact dermatitis, atopic dermatitis, psoriasis, and carcinogenesis (Baroni *et al.*, 2012).

Recent epidemiological studies suggest that PM negatively affects human skin (Vierkötter *et al.*, 2010), and exacerbates preexistent skin diseases (Kim *et al.*, 2013). However, information regarding the toxicological mechanisms by which PM can impact on skin function is limited.

In vitro and *in vivo* studies have shown a variety of biological effects after CAPs exposures, not only in chronic but also after acute exposures (Gurgueira *et al.*, 2002). The mechanisms by which the PM exerts its detrimental effects are believed to involve oxidative stress and inflammation (Donaldson *et al.*, 2005), both important contributors to extrinsic skin aging (Schröder *et al.*, 2006).

Injury mechanisms after PM exposure have been suggested to involve local reactive O_2 species (ROS) production which could, in part, be generated from the particles themselves. Moreover, smaller particles provide a higher surface area, in which different compounds could be adsorbed (Nel *el al.*, 2006). On the one hand, the oxidative capacity of PM has been attributed to its transition metal constituents, which typically include Fe, V, Cr, Mn, Co, Ni, Cu, Zn, and Ti. Most of these metals can catalyze Fenton-like reactions and ROS, initiating oxidative damage mechanisms (Chen and Lippmann, 2011). On the other hand, particles can serve as organic compounds carriers like polycyclic aromatic hydrocarbons (PAHs), which are highly lipophilic, and capable of localizing in mitochondria contributing to the reported ROS production (Li *et al.*, 2003). Furthermore, O_2-derived free radicals may also be generated by the interaction of particle pollutants and their components, with cellular enzymes and organelles (Magnani *et al.*, 2013).

Regarding inflammatory responses, it has been observed that systemic proinflammatory cytokines, such as TNF-α and IL-6 became increased after exposures to PM (Marchini *et al.*, 2014). In skin tissues, an increased reactive O_2 production could stimulate a variety of cells to release pro-inflammatory mediators, leading to infiltration of activated neutrophils and phagocytic cells which are able to produce more free radicals (Pillai *et al.*, 2005).

Taking into account that oxidative stress and inflammation play a predominant role in air pollution toxicity, the aim of the present work was to evaluate the ability of CAPs to promote skin tissue oxidative damage, and assess the possible mechanisms involved in this process.

2. Materials and Methods

2.1. Experimental model

2.1.1. CAPs suspension. CAPs were employed as a recognized ambient PM and were generously provided by B. Gonzalez-Flecha. They were collected using the Harvard Ambient Particle Concentrator (HAPC), which concentrates ambient air particles in a size range of 0.1–2.5 μm for subsequent exposure (Harvard School of Public Health, Boston, MA, USA) (Siutas *et al.*, 1995). CAPs samples from this source have been previously characterized in terms of elemental composition (Gurgueira *et al.*, 2002; Ghelfi et al., 2010). PM suspension was freshly prepared by resuspending CAPs particles in sterile saline solution at a final concentration of 25 or 100 μg/mL, followed by 10 min incubation in an ultrasonic water bath (Goldsmith *et al.*, 1998).

2.1.2. Skin exposure. Reconstructed human epidermis (RHE) tissues were used as a skin tissue model. EpiDermTM Tissue Model has been purchased to MatTek (MatTek In Vitro Life Science Laboratories, Bratislava, Slovak Republic). They were kept at 37 °C in a humidified 5% CO_2 atmosphere in a maintenance medium provided by manufacturers until the exposure. Prior to PM exposure, media was aspirated and fresh media was added. For the exposure, 10 μL of PM suspension (25 or 100 μg/mL) was topically applied over the RHE in a single dose (0.5 or 2.0 $\mu g/cm^2$ respectively). Control tissue was exposed to 10 μL of the vehicle (PBS). In order to avoid excess tissue moistening, a minimum suspension volume to deliver the particles was used. After exposure, tissues were also kept at 37 °C in a humidified 5% CO_2 atmosphere in a maintenance medium. Measurements were made after 24 or 48 hrs exposure. Since no differences between 24 and 48 hrs PBS exposure were observed (controls), the samples were pooled and presented as Control group.

2.2. Cytotoxicity determination

After CAPs exposure, culture media was collected at different time points (24 hrs and 48 hrs). Cytotoxicity was determined by lactate dehydrogenase (LDH) release in the media,

measured by enzymatic assay: in the first step NAD^+ is reduced to $NADH/H^+$ by the LDH-catalyzed conversion of lactate to pyruvate; in the second step the catalyst (diaphorase) transfers H/H^+ from $NADH/H^+$ to tetrazolium salt which is reduced to formazan. The amount of LDH in the supernatant were determined and calculated according to kit supplier's instructions (EuroClone Milan, Italy). All tests were performed in triplicate. Results are expressed as percentage of change relative to control values.

2.3. PM scanning electron microscopy (SEM)

The size, morphology and composition of CAPs were analyzed by SEM. To characterize the PM used, the grid was coated with dry CAPs or a drop of CAPs suspension was air dried onto a carbon film coated SEM grid and assessed in a scan electron microscopy (Zeiss EVO 40). Three different gates were selected in each grid to performed energy-dispersive X-ray spectroscopy (EDS) at variable pressure (XVP SEM), accelerating voltage 20kV. The INCA software was used for composition analysis (weight % and atomic %).

2.4. Hystochemistry

RHE tissue were fixed in 10% buffered formaldehyde and embedded in paraffin. For histological observation, the sections (4 µm thickness) were deparaffinized in xylene and rehydrated in alcohol gradients and then stained with hematoxylin and eosin (H&E).

The staining method involves application of hemalum, a complex formed from aluminum ions and hematein (an oxidation product of haematoxylin). Hemalum colors nuclei of cells blue. The nuclear staining is followed by counterstaining with an aqueous or alcoholic solution of eosin, which colors the eosinophilic structures in various shades of red, pink and orange.

2.5. Protein extraction

At each time point, skin tissues were washed with ice-cold PBS and lysed in ice-cold lysis buffer (20 mM Tris pH 8, 150 mM NaCl, 1% Triton X-100, 1 mM sodium orthovanadate, 1 µg/mL leupeptin, 1 µg/mL aprotinin, 1 µg/mL pepstatin, 10 µg/mL PMSF and 5 mM β-

glycerophosphate) (Sigma, Milan, Italy). The suspensions were centrifuged at 13,500 rpm for 15 min at 4 °C, the pellet were discarded and the supernatants were collected. Protein concentration was determined by the method of Bradford (Biorad, Milan, Italy).

2.6. 4-hydroxynonenal (4-HNE) assay

Lipid peroxidation of RHE exposed to CAPs was evaluated by measuring 4-hydroxynonenal (4-HNE) levels using a commercially available kit (BioSource, Milan, Italy). Briefly, protein extracted from the RHE, were used as samples for the measurement of 4-HNE protein adduct, which was conducted as manufacturer's introduction. The measured amount of 4-HNE protein adduct was normalized with protein concentration measured with the Bradford method. A calibration curve was performed using 4-HNE standard. Results are expressed as μg 4-HNE/mg protein.

2.7. Immunofluorescence

Paraffin embedded tissue sections (3 μm) were deparaffinized and rehydrated. After antigen retrieval and blocking, as previously described (Valacchi *et al*., 2011), the slides were incubated with the following antibodies: rabbit anti-IsoPro F2α (Abcam, Cambridge, UK), rabbit anti-COX2 (Cell Signaling Technology, Danvers, MA, USA), rabbit anti- p65 subunit (SantaCruz Biotechnologies, Inc, California, USA.) Then, the slides were incubated with fluorochrome-conjugated secondary antibodies (goat anti-rabbitAlexa Fluor 488; Thermo Fisher Scientific Inc.). The nuclei were counterstained by incubating the sections with 4′,6-diamidino-2-phenylindole (DAPI). Slides were mounted with Antifade. Negative controls were generated by omitting the primary antibody. Images were acquired and analyzed with a microscope Leica AF CTR6500HS (Microsystems) and analyzed with Image J software.

2.8. CYP1 expression

30 μg boiled proteins were loaded onto 10% sodium dodecyl sulphate–polyacrylamide electrophoresis gels and separated by molecular size. Gels were electro-blotted onto nitrocellulose membranes and then blots were blocked for 1 hr in Tris-buffered saline, pH 7.5,

containing 0.5% Tween20 and 3% milk. Membranes were incubated overnight at 4 °C with the appropriate primary antibodies: CYP1A1 (Cell Signalling; Celbio, Milan, Italy), β-actin (Cell Signalling; Celbio, Milan, Italy). The membranes were then incubated with horseradish peroxidase-conjugated secondary antibody for 1 hr, and the bound antibodies were detected by chemiluminescence (BioRad, Milan, Italy). β-actin was used as loading control. Images of the bands were digitized and the densitometry analysis was performed using Image-J software. Results are expressed as relative to β-actin expression.

2.9. IL-1 levels

IL-1α content was determined in the RHE culture media collected at different time points (24 or 48 h), using an ELISA kit (Thermo Scientific, Milan, Italy). It was done according to the manufacturer's instructions. The optical absorbance was measured with a microplate reader at 450 nm and correction at 530 nm. A calibration curve was performed using Recombinant Human IL-1α as standard. Results are expressed as pmol IL-1 α/mL.

2.10. TUNEL assay

The terminal deoxynucleotidyl transferase-mediated deoxyuridine triphosphate nick end labelling (TUNEL) assay was used to detect apoptotic nuclei in the epidermis. The TUNEL staining assay kit (Apo-BrdU-IHC In Situ DNA Fragmentation Assay, BioVision, Inc., Milpitas, CA) and all associated procedures were performed according to the manufacturer's instruction booklet. Briefly, skin tissues were fixed in 10% neutralized formalin and embedded in paraffin. Serial sections were deparaffinized, rehydrated, and incubated for 20 minutes at 37° C with proteinase K working solution (15 g/ml in 10 mM Tris-HCl, pH 7.5). After being rinsed twice with PBS, slices were incubated in hydrogen peroxide block for 10 minutes, and then 50 µL TUNEL reaction mixtures were added on the slices. Slices were incubated for 60 minutes at 37°C in a humidified atmosphere in the dark. After being rinsed with PBS, slices were added to 50 µL of converter-peroxidase and incubated in a humidified chamber for 30 minutes at 37 °C, and then 50 µL of diaminobenzidine substrates was added and the slices were

incubated for 10 minutes at 25 °C. After being rinsed with PBS, slices were analyzed under a light microscope. Cells with shrunken brown-stained nuclei were considered positive.

2.11. Tissue ultrastructural analysis

RHE morphology was evaluated by transition electron microscopy (TEM). Tissues were fixed with 2.5% glutaraldehyde in 0.1 M sodium cacodylate buffer for 4 hr at 4 °C. They were then washed with 0.1 M cacodylate buffer (pH 7.4) three times and post-fixed in 1% osmium tetroxide and 0.1 M cacodylate buffer at pH 7.4 for 1 hr at room temperature. The specimens were dehydrated in graded concentrations of ethanol and embedded in epoxide resin (Agar Scientific, 66A Cambridge Road, Stanstead Essex, CM24 8DA, UK). RHE were then transferred to latex modules filled with resin and subsequently thermally cured at 60 °C for 48 hr. Semi-thin sections (0.5-1 μm thickness) were cut using an ultra-microtome (Reichard Ultracut S, Austria) stained with toluidine blue, and blocks were selected for thinning. Ultra-thin sections of about 40-60 nm were cut and mounted onto formvar-coated copper grids. These were then double-stained with 1% uranyl acetate and 0.1% lead citrate for 30 min each and examined under a transmission electron microscope, (Hitachi, H-800), at an accelerating voltage of 100 KV.

2.12. Statistical analysis

Results were expressed as mean value ± SEM and represent the mean of triplicate determinations obtained in four separate experiments. ANOVA followed by Student–Newman–Keuls test was used to analyze differences among multiple experimental groups. Statistical significance was considered at $p < 0.05$.

3. Results

3.1. Cytotoxicity determination

As a first approach to evaluate the adverse effects of PM on skin tissues, LDH release measurements were carried out on RHE maintained media collected after different time points and CAPs doses exposure. As it is shown in Fig.1A, tissues exposed to 25 µg CAPs/mL presented increased LDH release only after 48 hrs (47%; $p < 0.05$), while RHE exposed to 100 µg CAPs/mL showed a significantly increased LDH release already at 24 hrs ($p < 0.01$) and continue up to 48 hrs ($p < 0.001$) after particles exposure when compared to control tissues (48% and 67% increased respectively).

3.2. CAPs characterization

Since CAPs exposure was able to induce skin tissues toxicity (Fig.1A); we performed CAPs characterization in regards to their morphology and composition by SEM. Elements present in CAPs samples are in accordance with previous description (Gurgueira *et al.*, 2002). As it is shown in Table 1, transition metals, mainly Fe, were observed through EDS analysis, and SEM image of CAPs showed that particles size is less than 10 µm (Figure 1B). Therefore, they can be categorized as fine ($PM_{2.5}$, aerodynamic diameter ≤ 2.5 µm) and ultrafine particles (UFP, aerodynamic diameter ≤ 0.1 µm).

3.3. Hystochemistry

As it is depicted in Fig. 1D, in all samples, the basal, spinous, granulous and cornified epidermal layers were present. The treated epidermis did not show morphological alterations. In fact, there were no relevant differences among the groups (controls, 24 hrs and 48 hrs-treated epidermis), although, after 24 h, mitoses in the basal layer were more easily found than 48 h after the treatment and in controls. However, the mitotic index (number of mitoses among 100 basal keratinocytes) did not significantly differ among the three groups.

3.3. Oxidative damage markers

One of the mechanisms suggested by which PMs exert adverse health effects is the oxidative stress occurrence, which may lead to lipid peroxidation. The F_2-α isoprostanes and 4-HNE levels are two of the most reliable oxidative damage markers. Isoprostanes are the product of arachidonic acid oxidation initiated by free radicals. As it is shown in Figure 2A, F_2-α isoprostanes levels, assessed by IsoPro F_2-α immunofluorescence integrate density, were clearly increased compared to the control group (control: 102 ± 1 IF), in the group exposed to 25 µg CAPs/mL for 48 hrs (52%) and RHE exposed to 100 µg CAPs/mL presented increased levels not only after 24 hrs (48%) exposure, but after 48 hrs (89%) as well ($p < 0.001$). In addition, both CAPs doses in RHE exposed for 48 hrs resulted significantly increased when compared to their dose matching groups exposed for 24 hrs ($p < 0.001$).

Regarding 4-HNE evaluation, another widely used phospholipid oxidative damage marker, only tissues exposed to 100 ug CAPs/mL for 24 h and 48 hrs presented a 28% ($p < 0.001$) and 20% ($p < 0.01$) respectively increase of phospholipid oxidation levels in comparison with control values (control: 0.25 ± 0.01 µg 4-HNE/mg prot.) (Figure 2B).

NFkB is a redox sensitive transcription factor that once activated, translocates to the nucleus where can trigger the gene expression of inflammatory mediators. To evaluate if CAPs were able to activate this pathway, subunit p-65 immunohistochemistry was performed in RHE exposed to PM, and positive stained nuclei percentage was assessed as NFkB activation parameter. As it is shown in Figure 2C, while no NFkB activation was observed in control RHE, CAPs exposure groups presented p-65 positive nuclei (25 µg CAPs/mL for 24 hrs: 28%; 25 µg CAPs/mL for 48 hrs: 26%; 100 µg CAPs/mL for 24 hrs: 32%; 100 µg CAPs/mL for 48 hrs: 38%).

3.5. CYP1A1 expression

In order to evaluate the effects of PM exposure on cytochrome P450 hemoproteins, CYP1A1 expression was assessed by Western blot. CYP1A1 protein is a cytochrome P450 enzyme superfamily member which is involved in xenobiotics metabolism. Skin tissues exposed to 25 µg CAPs/mL for 24 hrs presented a 73% increased expression ($p < 0.01$) compared to control values (control: 1.5 ± 0.3 CYP1A1/β-actin ratio). None of the other CAPs-exposed groups showed changes relative to control (Figure 2D).

3.6. Inflammation markers

The IL-1 isoforms play a key role in the inflammatory response trigger by air pollutants. Among them, IL-1α has been associated with pro-inflammatory mechanisms. IL-1α released by skin tissues after CAPs treatment was measured by a spectrophotometric assay, using RHE maintenance media as samples. Results are presented in Figure 3A. Every CAPs experimental group showed IL-1α levels significantly higher than the group exposed to PBS. PM-exposed groups comparison showed time point's differences. RHE treatment with CAPs presented higher values 48 hrs in relation to 24 hrs exposed of the same dose ($p < 0.01$).

PM-adverse health effects could also initiate inflammatory and signaling pathways where COX-2 is involved. Moreover, the expression of this enzyme is regulated by inflammatory mediators such as IL-1α. Therefore, it seems relevant to assess COX-2 expression through immunofluorescence. As it can be seen in Figure 3B, compared to control values, immunofluorescences integrate density quantification results significantly higher in CAPs groups regardless dose or time exposure. 48 hrs exposure to CAPs produce increased expression in comparison with 24 hrs group only after the lower dose exposure ($p < 0.001$).

3.7. DNA alterations

PM-generated oxidative metabolism and inflammatory mediators may also modulate genes involved in the control of the cell cycle and apoptosis and direct DNA alterations. As it

can be observed in Figure 4 through TUNEL assay, no signal could be detected in control RHE, while every CAPs-exposed tissue showed TUNEL positive nuclei, indicating double and single-stranded DNA fragmentation resulting from apoptotic signaling cascades.

3.8. Tissue ultrastructural analysis

With the aim of clarifying the interactions between CAPs and skin tissue ultrastructural analysis by TEM was performed. Interestingly we observed particles inside the tissue after 100 µg CAPs/mL. Slices from 24 hrs exposed RHE presented CAPs in the upper cell, near corneous layer, whereas 48 h after PM treatment particles were also found in deeper cell layers (Figure 5).

Discussion

Several researchers have established a direct correlation between increased environmental air PM levels and adverse health effects (Dominici *et al.*, 2006). People may be exposed to different air pollutants via inhalation, ingestion and dermal contact. Nowadays, epidemiological and clinical studies are progressively more interested in skin outcomes after PM exposure (Drakaki *et al*., 2014; Ahn, 2014). However, scarce data is available regarding the mechanisms exerted by air pollution on cutaneous tissues. In this scenario, the aim of the present study was to clarify the phenomena underlying the toxic pathways initiated by CAPs exposure in cutaneous tissues and to do so we have performed experiments in a tree dimensional skin culture model (RHE).

Our data show that CAPs exposure significantly affected RHE viability, as demonstrated by LDH release. Although, there was a dose-time relationship since when RHE were exposed to the lower dose of particles, skin tissues required more time to develop cytotoxicity. It is accepted that exposure to air pollution PM triggers an inflammatory response, endothelial activation and oxidative stress (Chen and Lippmann, 2009). Injury to diverse organs after air pollution contact has been suggested to be generated not only from the particles themselves, but mainly from the chemicals coated on their surface. Therefore, particles physical properties characterization becomes relevant. Concerning PM size, we found that CAPs are included in the fine and ultrafine groups considering the aerodynamic diameter observed (< 2.5 µm). Thanks to their small size but large surface per unit mass, they become highly reactive in biological surfaces and structures (Donaldson *et al*., 2005). The smaller the particles are, the higher is the diameter/surface area rate where molecules could be adsorbed. Therefore, fine and ultrafine particles fraction seem to be of major concern from the health perspective (Delfino *et al*., 2005). PM can act as carrier of both organic and inorganic compounds found in the particle's core. In agreement with previous CAPs characterization (Gurguereira *et al.*, 2002; *Ghelfi et al.*, 2010) we also observed the presence of transition

metals, such as Fe, in the surface of the PM. Due to their ability to participate in Fenton-like reaction, Fe could contribute to an increase of ROS production, which in turn, might be able to initiate molecular mechanisms leading to oxidative damage within the tissue. Besides transition metals, other compounds present in air pollution, such as semi-quinones, lipopolysaccaride, hydrocarbon, and ultrafine constituents, may also exert oxidative stress by presenting or by stimulating the cells to produce ROS. The augmented oxidant species production may overwhelm the enzymatic and non-enzymatic antioxidant defenses capacity, thus leading to deleterious effects (Bickers and Athar, 2006). Phospholipids are the macromolecules more sensitive to changes in the redox cellular status after PM exposure (Magnani *et al.*, 2011). CAPs exposure showed increased levels of arachidonic acid oxidation, as seen by IsoPro F_2-α immunofluorescence. The arachidonic acid once is oxidized, forms other radical compounds, which are able to increase the phospholipid oxidation and lead to further omega-6 PUFA oxidation as demonstrated by the increased levels of 4-HNE.

In addition to the above observations, it is accepted that oxidative stress is also involved in triggering pro-inflammatory pathways by activating redox sensitive transcription factors such as NFkB , that can contribute to the deleterious effects of PM in multicellular organisms (Marchini *et al.*, 2014). Once activated, NFkB can translocate to nucleus, as it is observed after CAPs exposure, and transcribes for several pro-inflammatory genes such as IL-1α and COX-1. Consistently, we have observed increase levels of the pro-inflammatory markers COX-2 and IL-1α in skin tissues exposed to PM.

Different hypothesis has been proposed concerning the initiation of the PM detrimental effects on cutaneous tissues. This could be due to an indirect effect by an outside-inside signaling cascade. As it has been mentioned, PM, especially smaller particles, may carry metal ions and/or organic compounds such as PAHs which are highly lipophilic and, both can penetrate the skin surface (Vierkotter *et al.*, 2014). Although it has been suggested that different air pollutants may have specific effects, it is worthily to observe that other pollutants like O_3,

which exert indirect toxic mechanism on skin (Valacchi *et al.*, 2002; Fortino *et al*. 2007), and recently has been showed that O_3 increased activation of the detoxifying enzyme cytochrome p450 via AhR receptor (Afaq *et al.*, 2009). This is in agreement with our observations in RHE PM-exposed tissues. Moreover PAHs are potent ligands for the AhR receptor, expressed by both keratinocytes and melanocytes, which upregulates pro-inflammatory mediators and increase ROS production (Fritsche *et al.*, 2007; Jux *et al.*, 2011).

On the other hand, PM-adverse health effects initiation involve penetration of PM into the skin. Nowadays it is accepted that increased levels of ambient PM, could enter skin either through hair follicles or trans-epidermally (Lademann *et al.*, 2004). Taking into account the physicochemical characteristics of CAPs it is clear that they are highly reactive toward biological surfaces. Their ability to disturb the skin barrier function relies on the amount of particles in touch with the corneocytes and the exposure period of time. According with the ultrastructural analysis only higher doses of CAPs can break through the stratum corneum and be found in deeper cell layers 48 h after exposure.

However, it is interesting that regardless the initiation mechanisms, the present PM exposure model, triggers apoptosis occurrence in every group treated, which means that CAPs leads to skin damage associated with the development of various skin diseases (Valacchi *et al.*, 2012).

In the present study we provide evidence that PM develop cutaneous damage not only directly, once particles reach deeper layers in the epidermis, but also indirectly, triggering a signaling pathway. Oxidative stress and an inflammatory response seems to be important steps in the CAPs-toxic mechanisms.

In conclusion, the relevant results showed in the present study provides new insights that are able to highlight the possible mechanism involved in PM exert detrimental skin effects.

Acknowledgment

The authors are thankful to Mr. Andrea Margutti for technical assistance.

References

Afaq, F., Zaid, M.A., Pelle, E., Khan, N., Syed, D.N., Matsui, M.S., Maes, D. and Mukhtar, H. (2009) Aryl hydrocarbon receptor is an ozone sensor in human skin. *J Invest Dermatol.* **129**(10), 2396-403.

Ahn, K. (2014) The role of air pollutants in atopic dermatitis. *J Allergy Clin Immunol.* **134**(5), 993-9.

Baroni, A., Buommino, E., De Gregorio, V., Ruocco, E., Ruocco, V. and Wolf, R. (2012). Structure and function of the epidermis related to barrier properties. *Clin. Dermatol.* **30**, 257– 262.

Bickers, D.R. and Athar, M. (2006) Oxidative stress in the pathogenesis of skin disease. *J Invest Dermatol.* **126**(12), 2565-75.

Brunekreef, B. and Holgate S.T. (2002). Air pollution and health. *Lancet* **360**, 1233–1242.

Chen, L. C., and Lipmann, M. (2009). Effects of metals within ambient air particulate matter (PM) on human health. *Inhal. Toxicol.* **21**, 1-31.

Delfino, R.J., Sioutas, C. and Malik, S. (2005) Potential role of ultrafine particles in associations between airborne particle mass and cardiovascular health. *Environ Health Perspect.* **113**(8):934-46.

Dominici, F., Peng, R.D., Bell, M.L., Pham, L., McDermott, A., Zeger, S.L. and Samet, J.M. (2006) Fine particulate air pollution and hospital admission for cardiovascular and respiratory diseases. *JAMA.* 295(10), 1127-34.

Donaldson, K., Tran, L., Jimenez, L. A. Duffin, R., Newby, D. E., Mills, N., MacNee, W. and Stone, V. (2005). Combustion-derived nanoparticles: a review of their toxicology following inhalation exposure. *Part. Fibre Toxicol.* **2,** 10.

Fortino, V., Maioli, E., Torricelli, C., Davis, P and Valacchi, G. (2007) Cutaneous MMPs are differently modulated by environmental stressors in old and young mice. *Toxicology Letters*

173, (2), 73-9.

Fritsche, E., Schäfer, C., Calles, C., Bernsmann, T., Bernshausen, T., Wurm, M., Hübenthal, U., Cline, J.E., Hajimiragha, H., Schroeder, P., Klotz, L.O., Rannug, A., Fürst, P.,Hanenberg, H., Abel, J. and Krutmann, J. (2007) Lightening up the UV response by identification of the arylhydrocarbon receptor as a cytoplasmatic target for ultraviolet B radiation. *Proc Natl Acad Sci U S A.* **104**(21), 8851-6.

Ghelfi E., Wellenius G. A., Lawrence J., Millet E. and Gonzalez-Flecha B. (2010) Cardiac oxidative stress and dysfunction by fine concentrated ambient particles (CAPs) are mediated by angiotensin-II. *Inhal Toxicol.* **22(11)**, 963–972.

Ghio, A. J., and Huang Y. C. (2004). Exposure to concentrated ambient particles (CAPs): a review. *Inhal. Toxicol.***16(1)**, 53-59.

Goldsmith, C. A., Imrich, A., Danaee, H., Ning, Y. Y. and Kobzik, L. (1998). Analysis of air pollution particulate-mediated oxidant stress in alveolar macrophages. J. *Toxicol. Environ. Health A* **54**, 529–545.

Gurgueira, S. A., Lawrence, J., Coull, B., Krisha Murthy, G. G. and González-Flecha, B. (2002)Rapid increases in the steady-state concentration of reactive oxygen species in the lungs and heart after particulate air pollution inhalation. *Environ. Health Perspect.* **110**, 749–755.

Jux, B., Kadow, S., Luecke, S., Rannug, A., Krutmann, J. and Esser, C. (2011) The aryl hydrocarbon receptor mediates UVB radiation-induced skin tanning. *J Invest Dermatol*. **131**(1), 203-10.

Kim, J., Kim, E. H., Oh, I., Jung, K., Han, Y., Cheong, H. K. and Ahn, K. (2013). Symptoms of atopic dermatitis are influenced by outdoor pollution. *J Allergy Clin Immunol* **132**, 495–497.

Krutmann, J., Liu, W., Li, L., Pan, X., Crawford, M., Sore, G. and Seite, S. (2014) Pollution and skin: from epidemiological and mechanistic studies to clinical implications. *J Dermatol Sci.* **76**(3):163-8.

Lademann, J., Otberg, N., Jacobi, U., Hoffman, RM. and Blume-Peytavi, U. (2005) Follicular penetration and targeting. *J Investig Dermatol Symp Proc.* **10**(3),301-3.

Li, N., Xia, T. and Nel, A. E. (2008). The role of oxidative stress in ambient particulate matter induced lung diseases and its implications in the toxicity of engineered nanoparticles. *Free Radic. Biol. Med.* **44,** 1689–1699.

Magnani, N.D., Marchini, T., Tasat, D.R., Alvarez, S. and Evelson, P.A. (2001) Lung oxidative metabolism after exposure to ambient particles. *Biochem Biophys Res Commun.* **412**(4), 667-72.

Magnani, N.D., Marchini, T., Vanasco, V., Tasat, D. R., Alvarez, S. and Evelson, P. (2013). Reactive oxygen species produced by NADPH oxidase and mitochondrial dysfunction in lung after an acute exposure to residual oil fly ashes. *Toxicol. Appl. Pharmacol.* **270**, 31–38.

Marchini, T., Magnani, N. D., Paz, M. L., Vanasco, V., Tasat, D., González Maglio, D. H., Alvarez, S. and Evelson, P. A, (2014). Time course of systemic oxidative stress and inflammatory response induced by an acute exposure to Residual Oil Fly Ash. *Toxicol. Appl. Pharmacol.* **274**, 274–282.

Nel, A. (2005). Atmosphere. Air pollution-related illness: effects of particles. *Science* **308**, 804–806.

Nel, A., Xia, T., Mädler, L. and Li, N. (2006). Toxic Potential of Materials at the Nanolevel. *Science* **311,** 622-627.

Pillai, S., Oresajo, C. and Hayward, J. (2005). Ultraviolet radiation and skin aging: roles of reactive oxygen species, inflammation and protease activation, and strategies for prevention of inflammation-induced matrix degradation—a review. *Int. J. Cosmet. Sci.* **27**, 17–34.

Schröder, P., Schieke, S. M. and Morita, A. (2006). Premature skin aging by infrared radiation, tobacco smoke and ozone. In Skin Aging. (B. A. Gilchrest, and J. Krutmann, Eds), pp 45–55. Springer-Verlag Editorial, New York, NY.

Sioutas, C., Koutrakis, P. and Burton, R. M. (1995). A technique to expose animals to concentrated fine ambient aerosols. *Envrion. Health Perpect.* **103**,172–177.

Valacchi, G., van der Vliet, A., Schock, B.C., Okamoto, T., Obermuller-Jevic, U., Cross, C.E. and Packer, P. (2002) Ozone exposure activates oxidative stress responses in murine skin. *Toxicology*. **179**, 163-170.

Valacchi, G., Lim, Y., Belmonte, G., Miracco, C., Zanardi, I., Bocci, V. and Travagli V. (2011) Ozonated sesame oil enhances cutaneous wound healing in SKH1 mice Wound Repair *Regen*. 19, 107–115.

Valacchi, G., Sticozzi, C., Pecorelli, A., Cervellati, F., Cervellati, C. and Maioli, E. (2012). Cutaneous responses to environmental stressors. *Ann NY Acad Sci* **1271**, 75–81.

Vierkötter, A., Schikowski, T., Ranft, U., Sugiri, D., Matsui, M., Kramer, U. and Krutmann J. (2010). Airborne particle exposure and extrinsic skin aging. *J. Invest. Dermatol.* **130**, 2719–2726.

World Health Organization (WHO). Burden of disease from the joint effects of Household and Ambient Air Pollution for 2012. Public Health, Social and Environmental Determinants of Health Department, WHO, 2014

Figure legends

Figure 1: Air pollution particles smaller than 2.5 μm increase skin tissue cytotoxicity. A) Cytotoxicity evaluation by LDH release in RHE maintenance media after 24 (□) or 48 h (▌) exposure to 25 or 100 μg CAPs/mL measured by an enzymatic assay. Data is presented as mean ± SEM, n ≥ 3.* $p < 0.05$; ** $p < 0.01$; *** $p < 0.01$ vs control group. B) CAPs morphology analysis. SEM image. 5000X. C) Skin tissue morphology evaluation by hematoxilin-eosin staining.

Figure 2: CAPs exposure increase oxidative damage occurrence and activation of transcription factor in skin tissue. A) Macromolecules oxidation measured by Isoprostanes levels in RHE slices (top panels) and their correspondent DAPI signal (lower panels) in i) control slices; ii) after 24 hrs exposure to 25 μg CAPs/mL; iii) after 48 hrs exposure to 25 μg CAPs/mL; iv) after 24 hrs exposure to 100 μg CAPs/mL; v) after 24 hrs exposure to 100 μg CAPs/mL. Integrated density quantification. *** $p < 0.001$ vs control group; ### $p < 0.001$ vs 24 h exposure to 25 μg CAPs/mL; ~~~ $p < 0.001$ vs 24 h exposure to 100 μg CAPs/mL group. B) Oxidative damage assessed through HNE content in RHE after 24 (□) or 48 hrs (▌) exposure to 25 or 100 μg CAPs/mL. Data is presented as mean ± SEM, n ≥ 3.* $p < 0.05$; *** $p < 0.01$ vs control group. C) NFκB nuclear translocation in RHE slices (top panels) and their correspondent DAPI signal (lower panels) in i) control slices; ii) after 24 hrs exposure to 25 μg CAPs/mL; iii) after 48 hrs exposure to 25 μg CAPs/mL; iv) after 24 hrs exposure to 100 μg CAPs/mL; v) after 24 hrs exposure to 100 μg CAPs/mL. Integrated density quantification. *** $p < 0.001$ vs control group; # $p < 0.001$ vs 24 hrs exposure to 25 μg CAPs/mL. D) CYP1A1 protein levels in RHE after 24 (□) or 48 hrs (▌) exposure to 25 or 100 μg CAPs/mL measured by Western blot. Data are presented as mean ± SEM, n ≥ 3.* $p < 0.05$ vs control group.

Figure 3: An inflammatory response is activated in skin tissue after CAPs exposure. A) IL-1 release in RHE maintenance media after 24 (□) or 48 hrs (▌) exposure to 25 or 100 μg CAPs/mL. Data are presented as mean ± SEM, n ≥ 3.* $p < 0.05$; ** $p < 0.01$ vs control group. B) COX2 protein levels in RHE slices (top panels) and their correspondent DAPI signal (lower panels) in A) control slices; B) after 24 hrs exposure to 25 μg CAPs/mL; C) after 48 hrs exposure to 25 μg CAPs/mL; D) after 24 hrs exposure to 100 μg CAPs/mL; E) after 48 hrs exposure to 100 μg CAPs/mL.

Figure 4: Oxidative and inflammatory mechanisms initiated after CAPs exposure lead to apoptotic cells in skin tissue. Apoptotic nuclei detection in RHE slices, evaluated by TUNEL assay in A) control slices; B) after 24 hrs exposure to 25 μg CAPs/mL; C) after 48 hrs exposure to 25 μg CAPs/mL; D) after 24 hrs exposure to 100 μg CAPs/mL; E) after 48 hrs exposure to 100 μg CAPs/mL.

Figure 5: CAPs are able to penetrate skin tissue. Ultrastructural analysis by TEM microscopy in RHE slices after 24 hrs exposure to 25 μg CAPs/mL; after 48 hrs exposure to 25 μg CAPs/mL; after 24 hrs exposure to 100 μg CAPs/mL; or after 48 hrs exposure to 100 μg CAPs/mL. A, B and C show magnification of their respective selected zones in the images, arrows point the zone were CAPs can be observed.

Table 1: CAPs composition evaluated by EDS analysis.

Element	Weight %	Atomic %
C	**44.89**	**22.60**
O	**38.40**	**35.70**
Mg	**0.15**	**0.09**
Al	**0.37**	**0.20**
Si	**14.75**	**7.81**
P	**0.20**	**0.10**
S	**0.55**	**0.25**
K	**0.11**	**0.04**
Ca	**0.34**	**0.13**
Fe	**0.23**	**0.06**
Total	**100.00**	

Figure 1

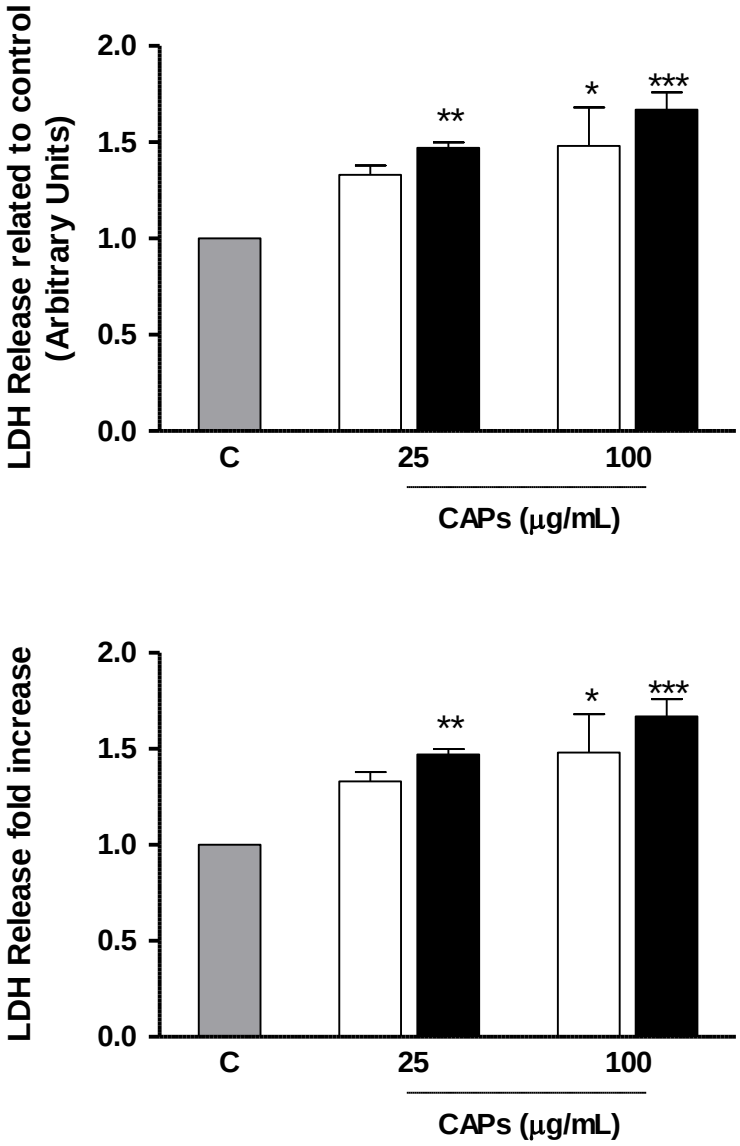
LDH Release related to control (Arbitrary Units)
2.0
1.5
1.0
0.5
0.0
**
*
***
C
25
100
CAPs (μg/mL)
LDH Release fold increase
2.0
1.5
1.0
0.5
0.0
**
*
***
C
25
100
CAPs (μg/mL)

Figure 2

A

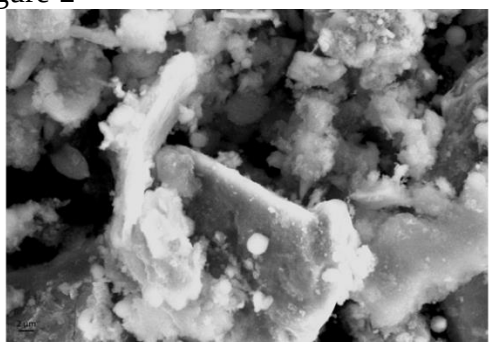

B

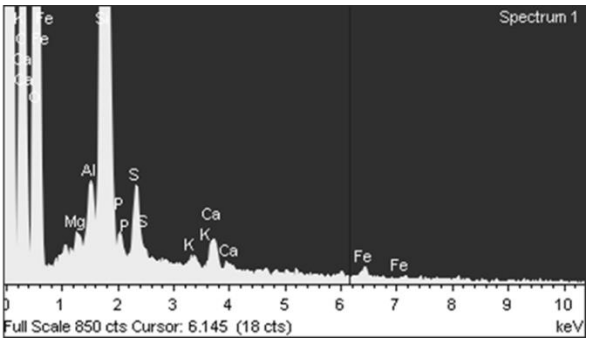
Spectrum 1
Fe
Al
S
Mg
P
P
S
K
Ca
K
Ca
Fe
Fe
0
1
2
3
4
5
6
7
8
9
10
Full Scale 850 cts Cursor: 6.145 (18 cts)
keV

Figure 3

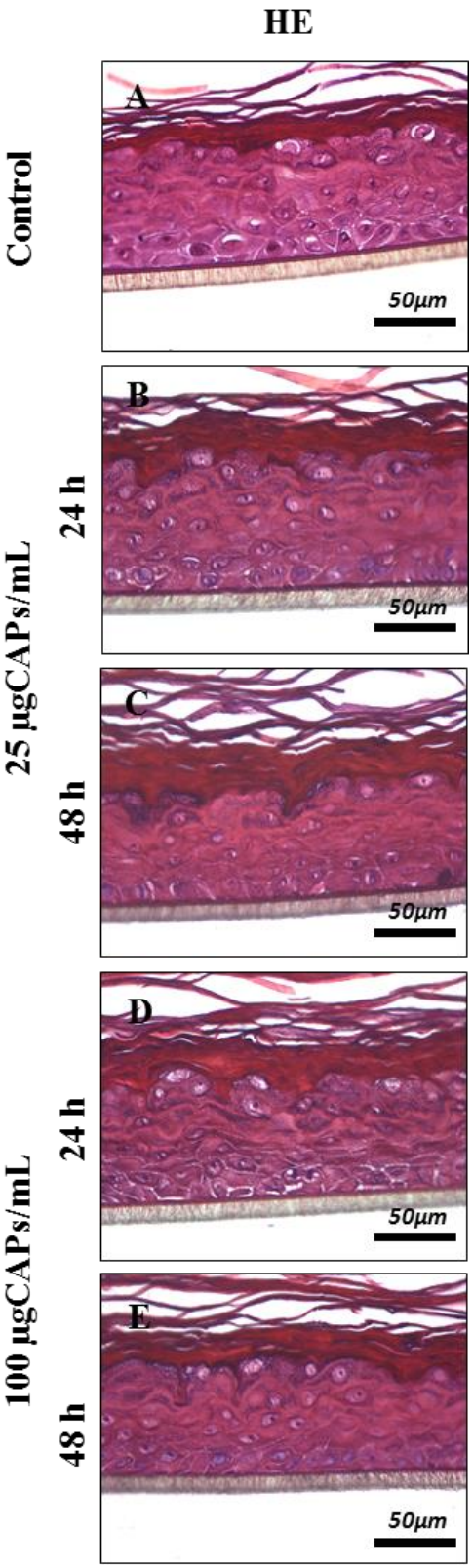
HE
Control
A
50μm
25 μgCAPs/mL
24 h
B
50μm
48 h
C
50μm
100 μgCAPs/mL
24 h
D
50μm
48 h
E
50μm

Figure 4

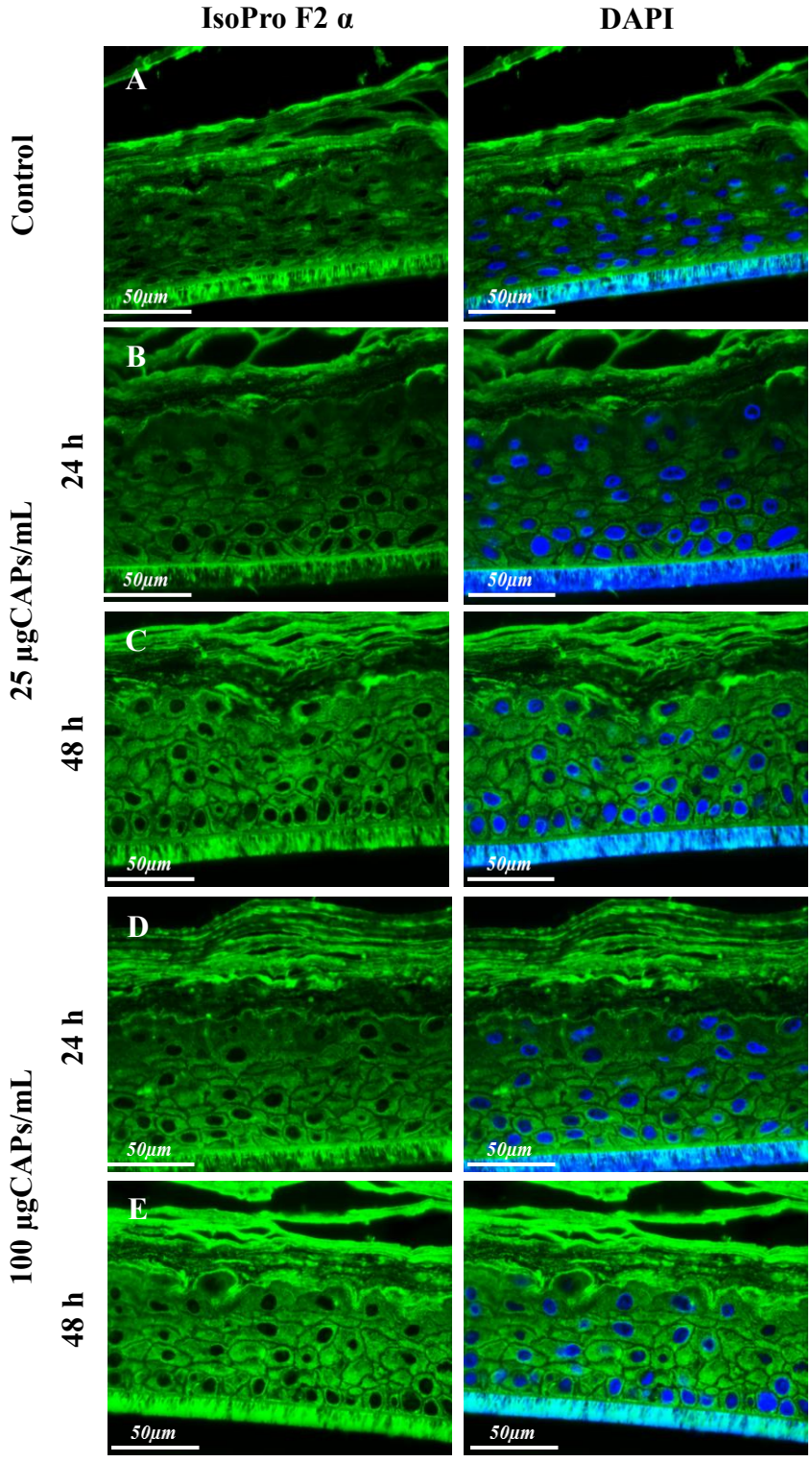
IsoPro F2 α
DAPI
Control
25 µgCAPs/mL
100 µgCAPs/mL
24 h
48 h
24 h
48 h
A
B
C
D
E
50µm

Figure 5

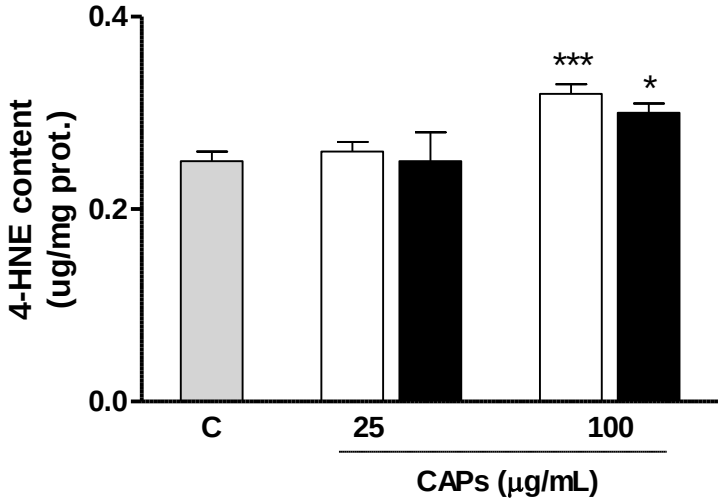

Figure 6

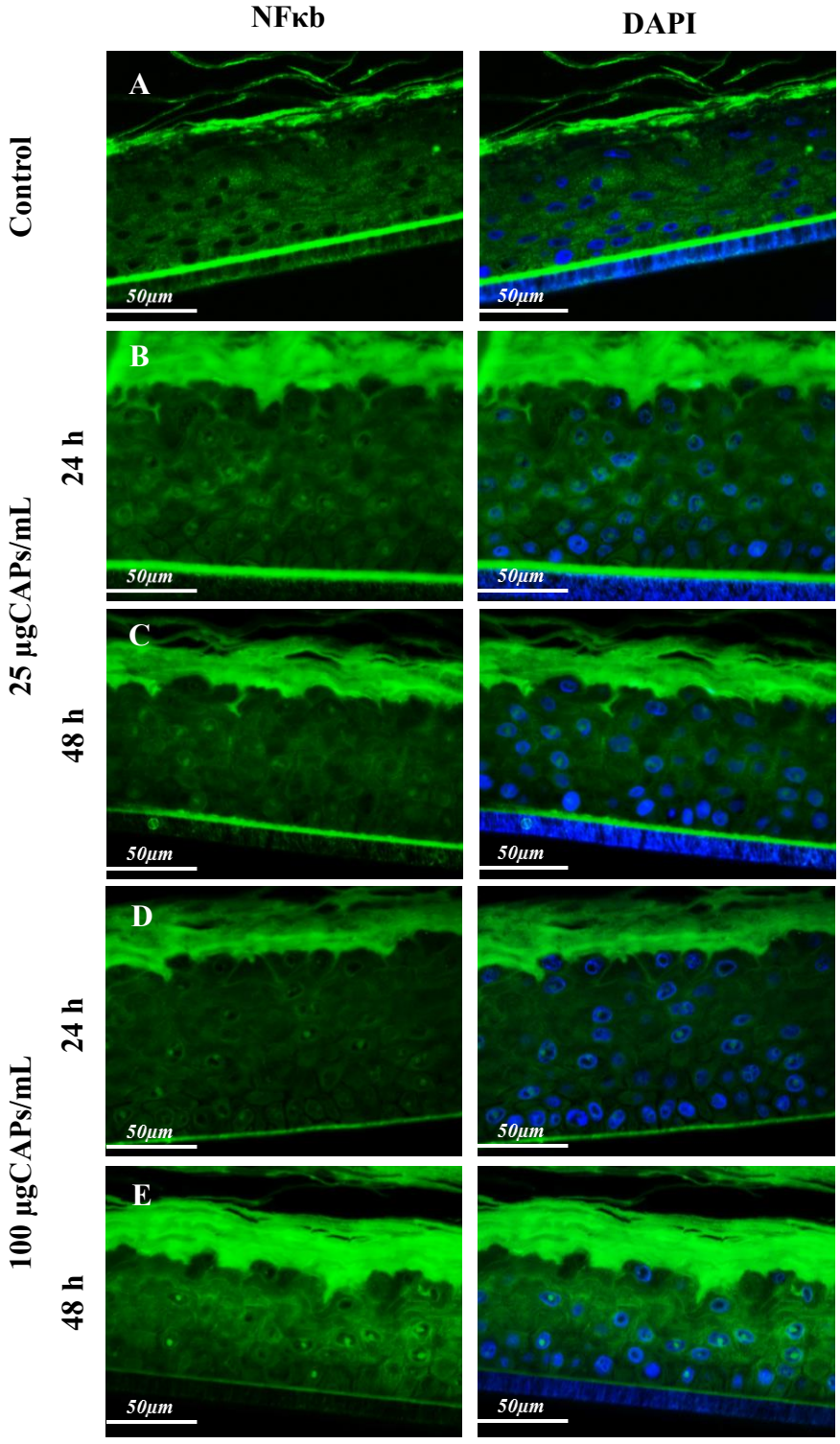
NFκb
DAPI
Control
A
50μm
25 μgCAPs/mL
24 h
B
C
48 h
100 μgCAPs/mL
D
E

Figure 7

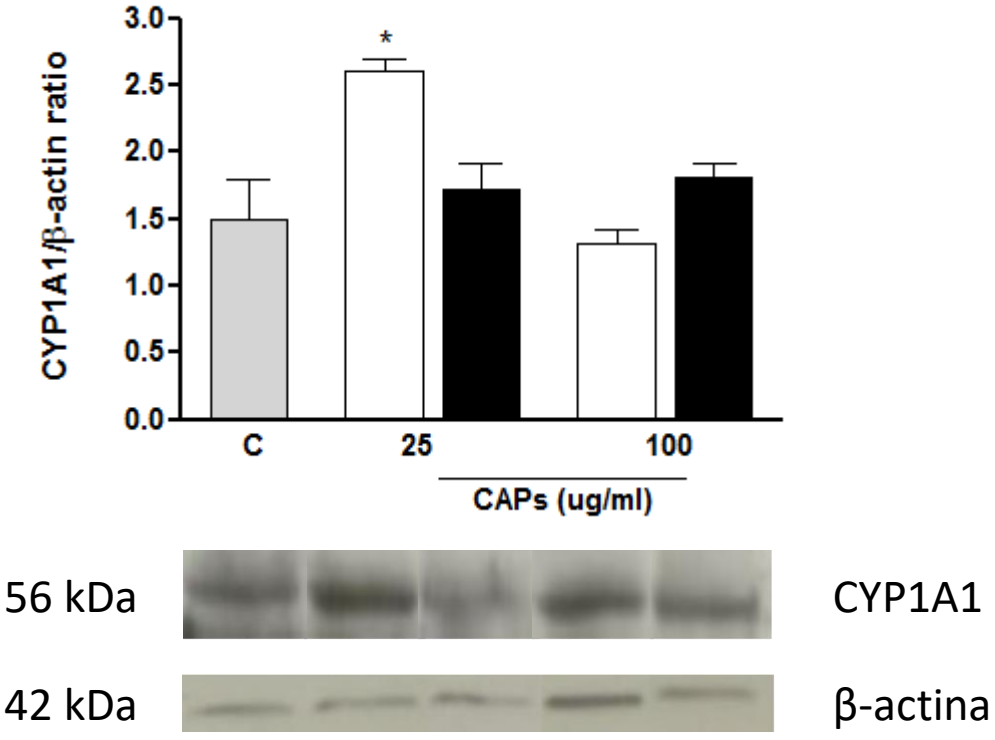
CYP1A1/β-actin ratio
3.0
2.5
2.0
1.5
1.0
0.5
0.0
*
C
25
100
CAPs (ug/ml)
56 kDa
CYP1A1
42 kDa
β-actina

Figure 8

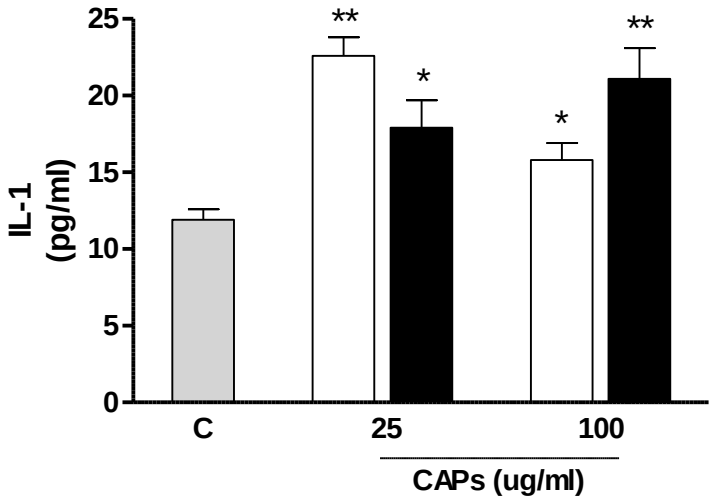

Figure 9

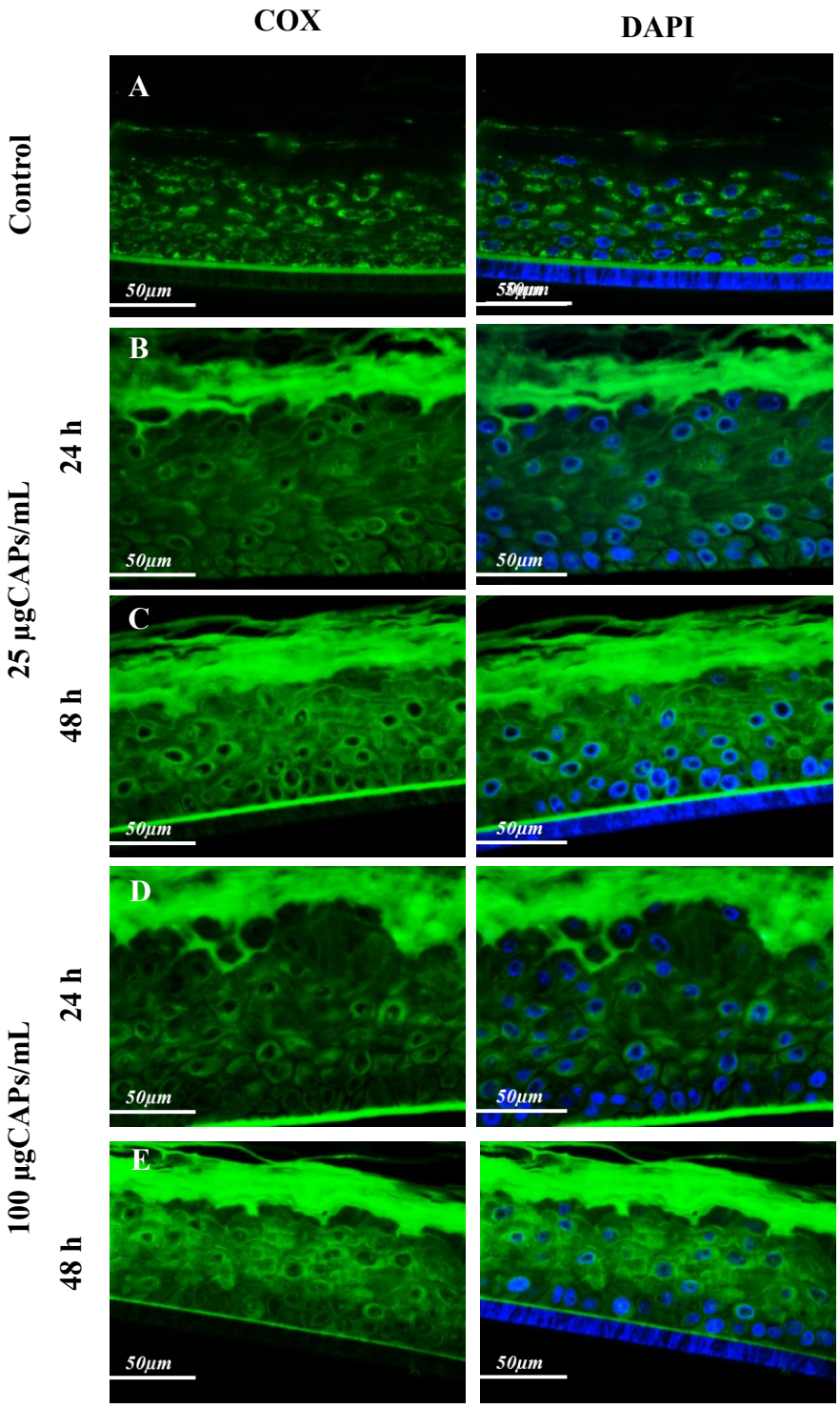
COX
DAPI
Control
A
50μm
25 μgCAPs/mL
24 h
B
50μm
48 h
C
50μm
100 μgCAPs/mL
24 h
D
50μm
48 h
E
50μm

Figure 10

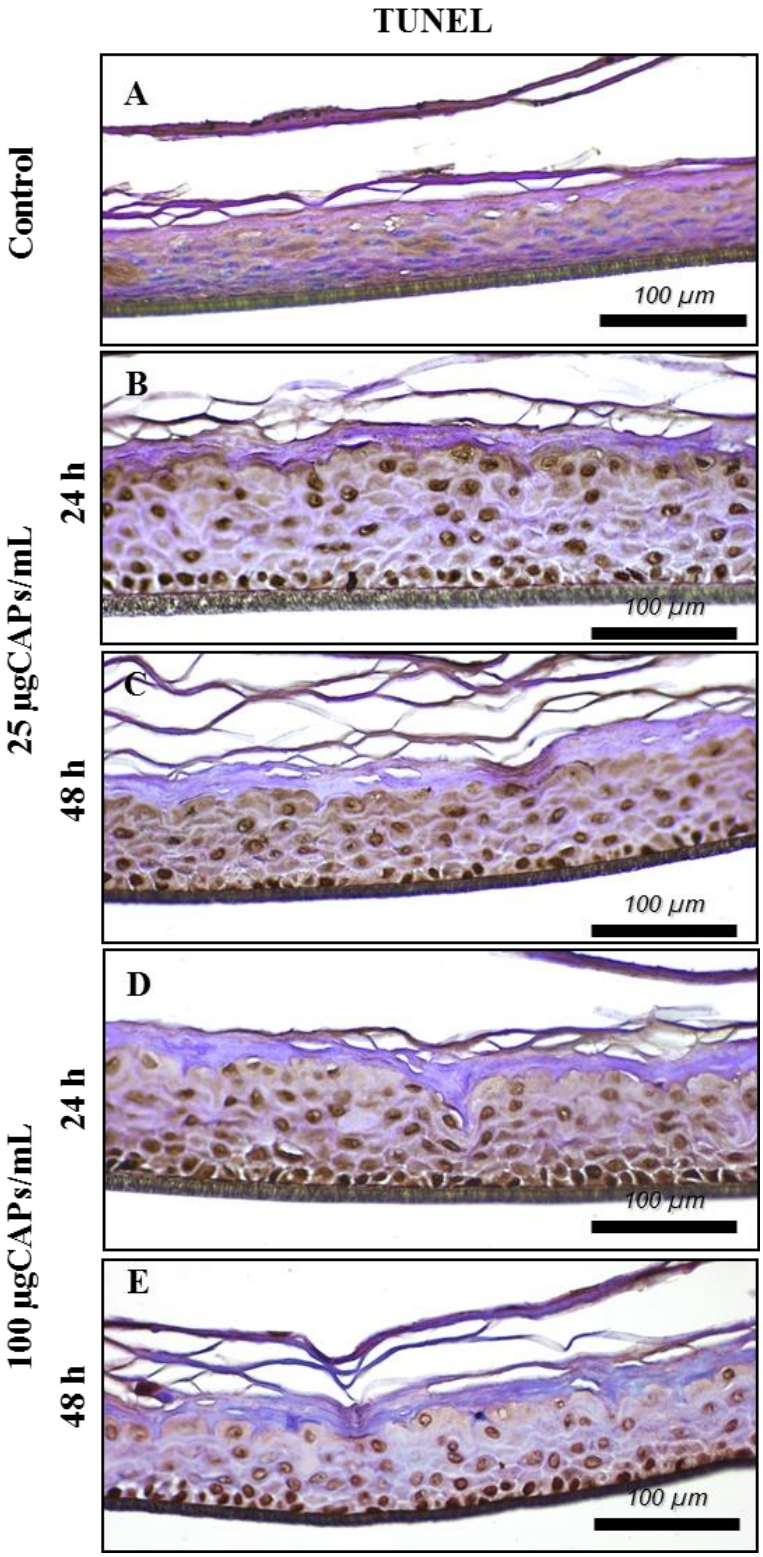
TUNEL
Control
A
100 µm
25 µgCAPs/mL
24 h
B
100 µm
48 h
C
100 µm
100 µgCAPs/mL
24 h
D
100 µm
48 h
E
100 µm

Figure 11

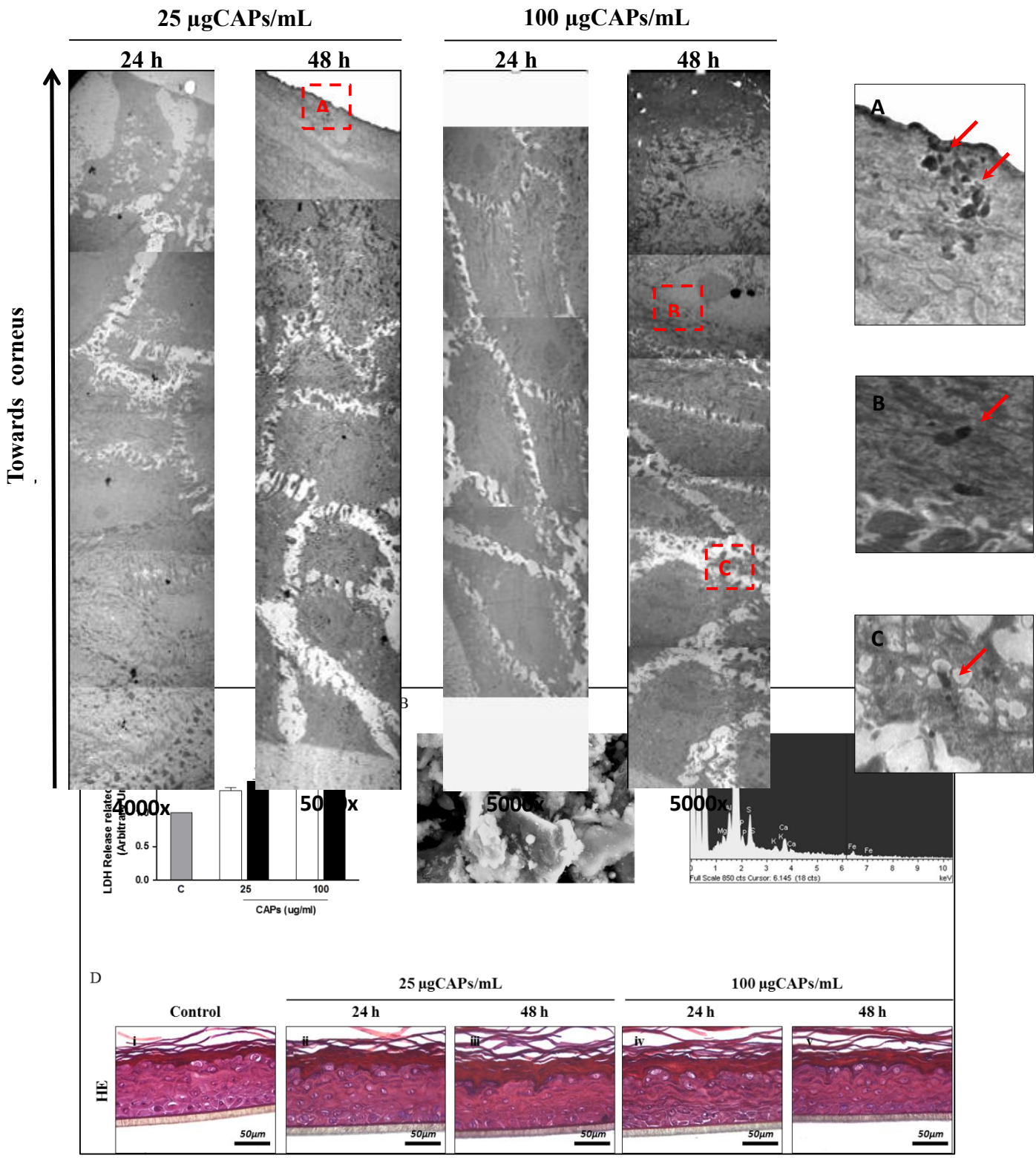

Figure 1: Air pollution particles smaller tan 2.5 µm increase skin tissue citotocicity. A) Cytotoxicity evaluation by LDH release in RHE maintenance media after 24 (□) or 48 h (■) exposure to 25 or 100 µg CAPs/mL measured by an enzymatic assay. Data is presented as mean ± SEM, n ≥ 3.* $p < 0.05$; ** $p < 0.01$; *** $p < 0.01$ vs control group. B) CAPs morphology con composition analysis. A) CAPs SEM image. 5000X. C) EDS spectrum

evaluated by INCA software. D) Skin tissue morphology evaluation by hematoxilin-eosin histochemistry.

Figura 2

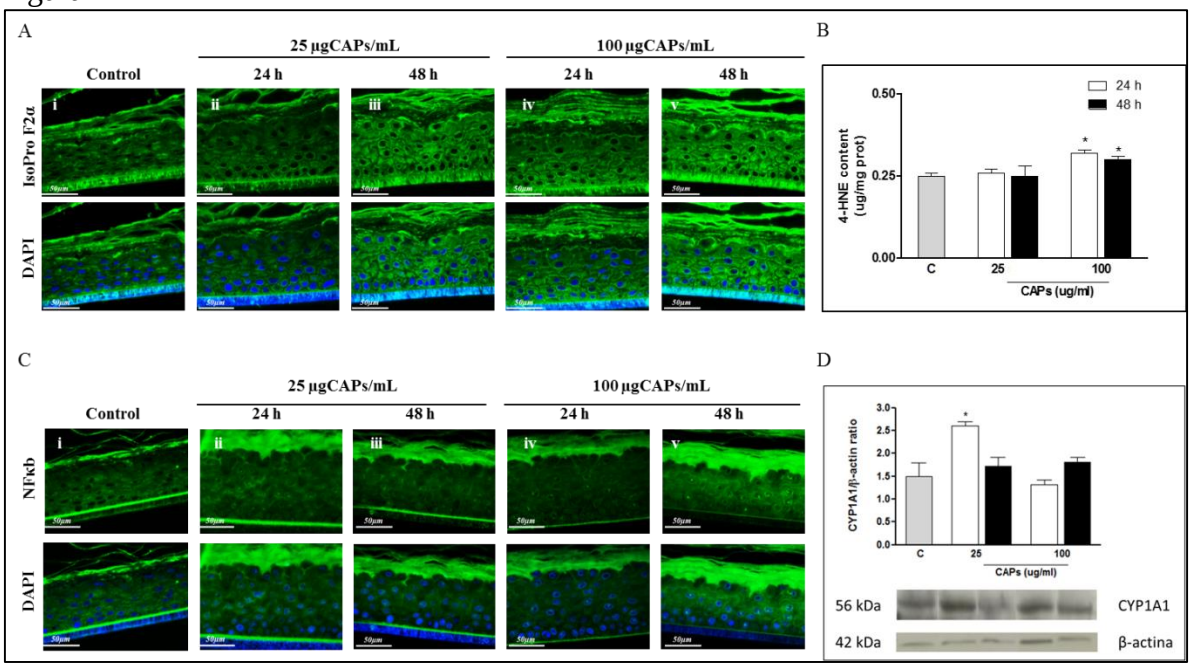

Figure 2: CAPs exposure increase oxidative damage occurrence and activation of transcription factor in skin tissue. A) Macromolecules oxidation measured by Isoprostanes expression in RHE slices (top panels) and their correspondent DAPI signal (lower panels) in i) control slices; ii) after 24 h exposure to 25 µg CAPs/mL; iii) after 48 h exposure to 25 µg CAPs/mL; iv) after 24 h exposure to 100 µg CAPs/mL; v) after 24 h exposure to 100 µg CAPs/mL. B) Oxidative damage assessed through HNE content in RHE after 24 (□) or 48 h (■) exposure to 25 or 100 µg CAPs/mL measured by an enzymatic assay. Data is presented as mean ± SEM, n ≥ 3.* $p < 0.05$; *** $p < 0.01$ vs control group. C) NFκb traslocation to nucleus in RHE slices (top panels) and their correspondent DAPI signal (lower panels) in i) control slices; ii) after 24 h exposure to 25 µg CAPs/mL; iii) after 48 h exposure to 25 µg CAPs/mL; iv) after 24 h exposure to 100 µg CAPs/mL; v) after 24 h exposure to 100 µg CAPs/mL. D) CYP1A1 expression in RHE protein extraction after 24 (□) or 48 h (■) exposure to 25 or 100 µg CAPs/mL measured by western blot. Data is presented as mean ± SEM, n ≥ 3.* $p < 0.05$ vs control group.

Figure 3

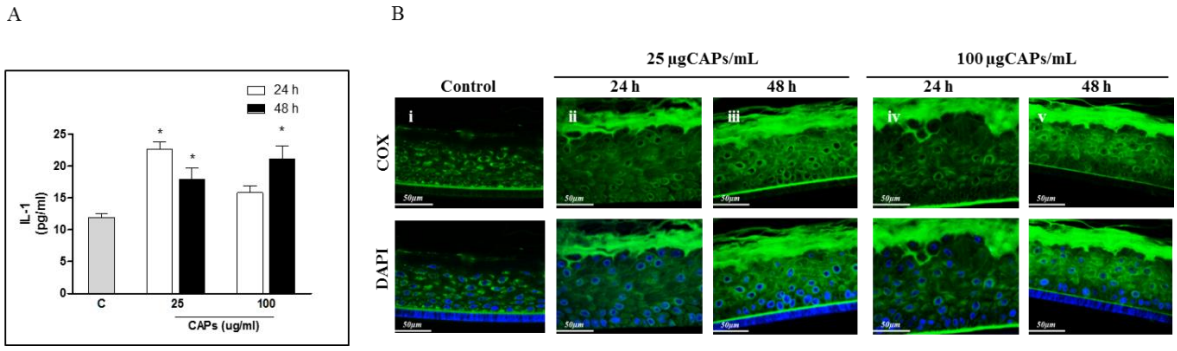

Figure 3: An inflammatory response is activated in skin tissue after CAPs exposure. A) IL-1 release in RHE maintenance media after 24 (□) or 48 h (■) exposure to 25 or 100 µg CAPs/mL measured by an enzymatic assay. Data is presented as mean ± SEM, $n \geq 3$.* $p < 0.05$; ** $p < 0.01$ vs control group. B) COX expression in RHE slices (top panels) and their correspondent DAPI signal (lower panels) in A) control slices; B) after 24 h exposure to 25 µg CAPs/mL; C) after 48 h exposure to 25 µg CAPs/mL; D) after 24 h exposure to 100 µg CAPs/mL; E) after 24 h exposure to 100 µg CAPs/mL.

Figure 4

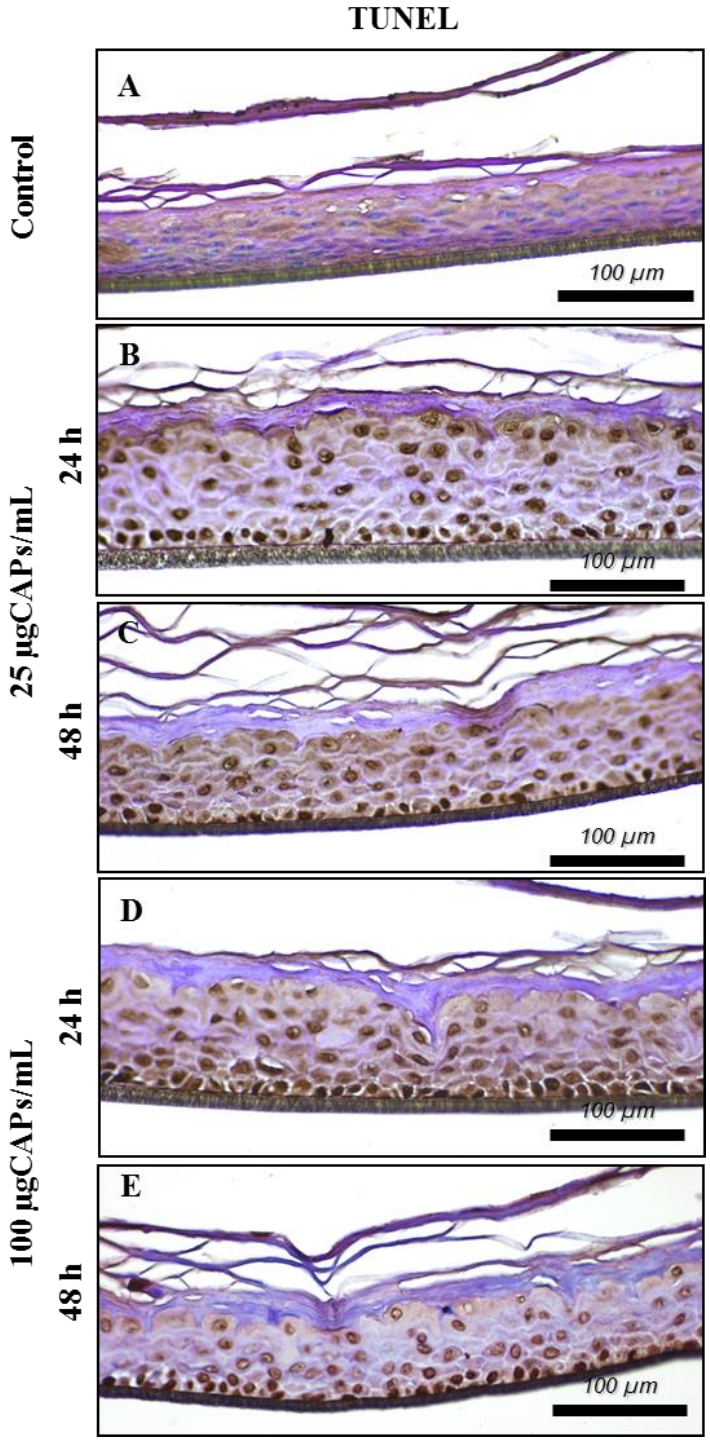

Figure 4: Oxidative and inflammatory mechanisms initiated after CAPs exposure lead to apoptotic cells in skin tissue. Apoptotic nuclei detection in RHE slices, evaluated by TUNEL assay in A) control slices; B) after 24 h exposure to 25 µg CAPs/mL; C) after 48 h exposure to 25 µg CAPs/mL; D) after 24 h exposure to 100 µg CAPs/mL; E) after 24 h exposure to 100 µg CAPs/mL.

Figure 5

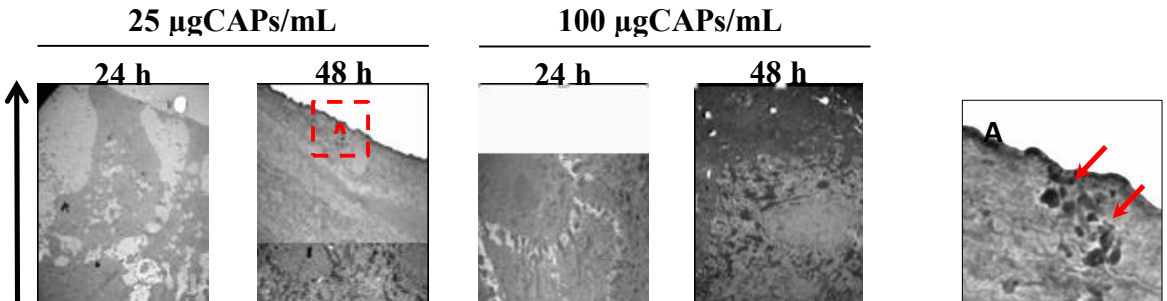

Figure 5: CAPs are able to penetrate skin tissue. Ultrastructural analysis by TEM microscopy in RHE slices after 24 h exposure to 25 μg CAPs/mL; after 48 h exposure to 25 μg CAPs/mL; after 24 h exposure to 100 μg CAPs/mL; or after 24 h exposure to 100 μg CAPs/mL. A, B and C show magnification of their respective selected zones in the images, arrows point the zone were CAPs can be observed.